CONF-790808--7

BNL-NUREG-26083

MASTER

HEAT REMOVAL CHARACTERISTICS OF VOLUME-HEATED BOILING POOLS WITH INCLINED BOUNDARIES IN BUBBLY FLOW REGIME*

G. A. Greene
Mechanical Engineer
Brookhaven National Laboratory
Upton, New York 11973

N. Abuaf
Mechanical Engineer
Brookhaven National Laboratory
Upton, New York 11973

O. C. Jones, Jr.
Mechanical Engineer
Brookhaven National Laboratory
Upton, New York 11973

C. E. Schwarz
Technical Specialist
Brookhaven National Laboratory
Upton, New York 11973

ABSTRACT

The heat transfer characteristics of volume-heated boiling pools are of importance in the safety analysis of hypothetical core disruptive accidents in liquid metal fast breeder reactors. Investigations into the heat transfer and hydrodynamic behavior of such volume-heated boiling pools have been few. The existing work in boiling pool heat transfer is reviewed, and current modeling efforts are described. The current experiment is discussed in detail, and significant improvements in experimental techniques are described. The data for local convective boundary heat transfer coefficient and pool-averaged void fraction are presented for the bubbly flow regime over a range of dimensionless power, j_{g_∞}/U_∞, up to unity, and wall angles of 90° (vertical), 75°, and 60°. The data are compared to existing correlations for local heat transfer and to a one-dimensional drift flux model for local and average void fraction.

It is shown that the drift flux model predicted the experimental data for average void fraction in the bubbly flow regime well when based upon the net boiling power. However, it was demonstrated that the existing correlations for local and average boundary heat flux (based on Gustavson's data) underpredicted the present data by as much as a factor of 2 or more.

NOMENCLATURE

a	Test plate thickness
C	Constant
C_o	Distribution parameter
g	Gravitational acceleration
Gr	Grashof number
h	Heat transfer coefficient
H	Height
h_{fg}	Heat of vaporization
j	Superficial velocity
j_{g_∞}	Superficial vapor velocity at pool surface
k	Thermal conductivity
K_i	Correlation coefficient
L	Length
n	Defined in Eq. 10
Nu	Nusselt number
P	Pressure
Pr	Prandtl number
$\dot{Q}$	Heat Flux
$\dot{Q}'''$	Volumetric power density
Ra	Rayleigh number

*Work carried out under the auspices of the United States Nuclear Regulatory Commission.

Re	Reynolds number
T	Temperature
U_∞	Terminal rise velocity of bubble
V	Velocity
V_{gj}	Drift velocity
x	Coordinate (along wall)
Y	Defined in Eq. 8
Z	Defined in Eq. 9
α	Void fraction
$\bar{\alpha}$	Average void fraction
β	Coefficient of thermal expansion
μ	Dynamic viscosity
ν	Kinematic viscosity
ρ	Density
θ	Wall angle from vertical
Γ_v	Volumetric vapor source
ξ	Normalized coordinate

ubscripts

B	Boiling
C	Forced convective
eff	Effective
f	Film
g	Gas
l	Liquid
N	Natural convective
o	Initial
TC	Thermal convective
v	Vapor
w	Wall
∞	Infinity
*	Modified

NTRODUCTION

The heat transfer characteristics of volume-eated boiling pools are of importance in the safety nalysis of hypothetical core disruptive accidents HCDA) in liquid metal fast breeder reactors (LMFBR). n general, these pools would be composed of molten uel and steel and would generate heat as a result of fission product decay. The fluid dynamic characteristics, as well as the containability of such boiling systems, would depend intimately on the heat loads applied to the surrounding boundaries. In addition, the thermodynamic and hydrodynamic states of the boiling mixture might determine the initial or boundary conditions for seperate but related phenomena, such as nuclear recriticality, structural integrity, flow and freezing of multiphase fluids, etc. Confidence in the conceptualization, as well as computation of such hypothetical events depends to a great deal upon the ability to predict the vapor generation rate, void fraction, and local boundary heat flux from such volume-boiling pools. It is the purpose of this paper to present new experimental data for local boundery heat transfer coefficients and average void fraction in volume-boiling pools and compare these results to previous experimental data, as well as to existing empirical models.

BACKGROUND

Numerous studies exist in the literature concerning heat transfer from liquid pools with an internal heat source. A brief review of this literature may be found in other sources [1,2] and will not be included here. However, investigations into the heat transfer and hydrodynamic behavior of volume-heated boiling pools have been few and none are known to exist prior to this decade.

The earliest known attempt to consider the heat transfer from volume-heated boiling pools is the work performed at Argonne National Laboratory by Stein, et al. [3]. In this work, a solution of NaCl and water was boiled in an open container by joule heating. The average downward and horizontal heat fluxes were measured by thermocouples soldered in small dead-end holes in tha plates making up the electrodes and base, and in the coolant system.

A model was presented which separated the boundary heat transfer into a natural convection and forced convection regime. The natural convection regime was shown to agree with the correlation below,

$$Nu_N = .677[Pr/(.952 + Pr)]^{1/4} Ra^{1/4} \qquad (1)$$

where $Nu_N = \dot{Q}_N x/(k\Delta T)$, $Ra = PrGr$, and $Gr = g\beta\Delta T x^3/\nu^2$. The forced convection regime was shown to be correlatad by the relation,

$$Nu_C = .664\ Pr^{1/3}\ Re^{1/2} \qquad (2)$$

where $Nu_C = \dot{Q}_C x/(k\Delta T)$ and $Re = V_B x/\nu$. Both relations are valid only for laminar flow conditions. For convenience, a thermal convection reference velocity, V_{TC}, was defined as

$$V_{TC} = (g\beta\Delta T x)^{1/2} = [g(\rho_w - \rho_\infty)x/\rho_f]^{1/2} \qquad (3)$$

and an equivalent free stream velocity, V_B, was defined as below;

$$V_B = 40\ \dot{Q}_B^{0.72} \qquad (4)$$

it was reported that for $V_B/V_{TC} \leq 0.2$, forced convection heat transfer was negligible and Eq. 1 applied. For $V_B/V_{TC} > 3.0$, thermal convection was negligible

and Eq. 2 applied. For values of V_B/V_{TC} intermediate to these values, mixed convection existed. The results of this investigation indicated that downward heat fluxes were found to be significantly larger than predictions from conduction theory would indicate; in addition, at the higher boiling heat fluxes, horizontal heat transfer was found to be significantly larger than values calculated by thermal convection alone, and could be correlated empirically by the laminar forced convection model.

The next attempt to experimentally characterize boundary heat transfer from volume-boiling pools was the work of Gabor, et al. [4] from Argonne National Laboratory. In their work, they used simulant solutions of $ZnSO_4$ in water. Base plates of two lengths (191 and 381 mm) and three electrode heights (64, 114, 230 mm) were used. The volumetric boiling power was supplied by joule heating as in the previous work. The electrodes and base plate were used as the heat transfer surfaces; thermocouples were buried halfway into the copper plates for temperature measurements, seven into the base plate, and two in each of the electrodes. Boundary heat losses were measured by calculating the enthalpy increase of the water coolant flowing in coils of copper tubing brazed to the backs of the electrodes. In these tests, the heat transfer rate to the vertical electrode was measured in two segments; for the 114 mm pool depth, the electrode was split into separately-cooled segments of 25 mm at the top and 89 mm at the bottom. For the 230 mm pool depth, the electrode was split into a 25 mm upper segment and a 205 mm lower segment. The opposite electrode was unsegmented and of the same overall length.

The ratios of the boundary heat fluxes, $\dot{Q}_{upper}/\dot{Q}_{lower}$, were investigated as a function of the boiling heat flux, $\dot{Q}_B$. It was found that for low boiling heat flux ($\dot{Q}_B$ less than 3.5 cal/sec cm^2 for the 230 mm pool; $\dot{Q}_B$ less than 6 cal/sec cm^2 for the 114 mm pool), the ratio $\dot{Q}_{upper}/\dot{Q}_{lower}$ was in the range of 1.5 to 2, in agreement with the prediction from thermal convection theory. For high boiling heat flux ($\dot{Q}_B$ greater than 4.5 cal/cm^2 sec for the 230 mm pool; $\dot{Q}_B$ greater than 9 cal/cm^2 sec for the 114 mm pool), the heat flux ratio was more nearly equal unity and equal to the heat flux to the unsplit electrode. The data was correlated in terms of a Nusselt number and Reynolds number based on the superficial vapor velocity. The Prandtl number was assigned separate exponential weight of 0, 1/3, and 1/2 powers. As a result, a new model was presented for horizontal heat flux based on bubble-induced laminar forced convection of the form

$$Nu = C\ Re^{1/2} \tag{5}$$

where the constant C included the effect of the Prandtl number and the superficial vapor velocity was defined as in Eq. 4.

While the studies reported so far have contributed to the understanding of some hydrodynamic and heat transfer processes occurring in internally heated boiling pools, they do not provide a mechanistic model for predicting local boundary heat transfer or void fraction in such pools. Recognizing this shortcoming, Gustavson, et al. [2] undertook an investigation into the local distribution of boundary heat transfer and void fraction in internally heated boiling pools. In their work, they also considered a rectangular pool of $ZnSO_4$ and water, joule heated by passing a-c current through the pool between two electrodes. Instead of using the electrode as the heat transfer surface, an instrumented test plate was installed, designed to allow measurement of local heat transfer to thermally isolated segments. Each segment was cooled by flowing water through separate cooling channels, and each flow rate was separately controlled to insure an isothermal pool-side surface temperature. The heat flux to each segment was measured by measuring the temperature rise and the flow rate of the coolant for each segment. The surface temperature of each segment was determined by extrapolating the interior thermocouple reading at the segment centerline to the test wall surface across 0.38 mm of aluminum and 0.76 mm Teflon sheet, which was cemented to the aluminum test wall surface for electrical insulation from the pool. A constant level weir was connected to an inlet at the pool bottom, which fed a steady flow of fluid to the pool to identically replace the losses due to vaporization. In this fashion, the net power for vaporization could be determined. The accuracy of the measured heat transfer coefficient in these tests was reported to be $\pm$ 40 percent.

The authors proposed that boundary heat transfer from volume-heated boiling pools was a mixed convection-type heat transfer phenomenon in which the effects were superimposable. They proposed, for laminar flow, that the thermal convective component be modeled as

$$Nu_N(x) = .42[Gr(x)Pr]^{0.25} \tag{6}$$

where Gr(x) was the local Grashof number based on the average pool film density difference, and $Nu_N(x)$ now represented the local natural heat transfer correlation where x was measured along the heat transfer surface downward from the free surface. The forced convective component was represented by

$$Nu_C(x) = .332\ Re(x)^{1/2}Pr^{1/3} \tag{7}$$

where Re(x) is the local Reynolds number based on the superficial vapor velocity at the pool surface. The method of modeling the combined natural/forced convection from a volume-boiling pool consisted of correlating the ratio

$$Y = \frac{Nu}{Nu_N} \tag{8}$$

to the group

$$Z = \frac{Nu_C}{Nu_N} \tag{9}$$

where Nu was the effective Nusselt number for the combined heat transfer process. Following a general correlation procedure, [5] it was suggested that the functional form of the correlation should be

$$Y = [1 + Z^n]^{1/n} \tag{10}$$

where n was determined by a best fit evaluation of the data. Alternate forms of Eqs. 6 and 7 were

proposed for the case of turbulent heat transfer. The correlation was tested against the measured average heat transfer data from their tests. The best agreement was obtained using the laminar relations and a value of n = 1.

ANALYTICAL MODELING

The data of Gustavson, et al. represent the first data available for local convective heat transfer coefficient from volume-heated boiling pools. The present authors conceived from the available data that the mode of heat transfer, instead of resembling mixed convection in which the effects were approximately superimposed, more closely approximated an enhanced mode of natural convection boundary layer flow and heat transfer [1]. The phenomenon of boundary layer flow and heat transfer is depicted in Fig. 1. It is assumed that the vapor rising through the pool causes a net liquid drift upward, which encounters the free surface and is forced to return downward along the cold boundary. In this case, the net bouyancy effect is due to the liquid-to-two-phase density difference. The heat transfer distribution from the volumetrically boiling pool to the boundary exibits behavior not unlike a single-phase natural convection boundary layer, enhanced by the flow of net liquid recirculation due to upward vapor drag through the central liquid and downward along the walls. With this point of view in mind, single-phase natural convection boundary layer theory coupled with the bouyancy affect of the two-phase flow in the bulk liquid was used to attempt to correlate the Nusselt number to a modified Rayleigh number.

The Grashof number may be written as [1]

$$Gr^*(x) = g_{eff}(\rho_w - \rho_\infty)\rho_f x^3/\mu_f^2 \tag{11}$$

where the density difference is

$$(\rho_w - \rho_\infty) = \rho_w - [(1-\alpha)\rho_{f\infty} + \alpha\rho_{v\infty}] \tag{12}$$

If it is assumed that $\alpha\rho_{v\infty} << (1-\alpha)\rho_{f\infty}$, this reduces to

$$(\rho_w - \rho_\infty) = \rho_w - (1-\alpha)\rho_{f\infty} \tag{13}$$

and Eq. 11 becomes

$$Gr^*(x,\alpha) = g_{eff}[\rho_w - (1-\alpha)\rho_{f\infty}]\rho_f x^3/\mu_f^2 \tag{14}$$

Furthermore, if the boundary is inclined from the vertical by an angle θ in such a manner that the boundary layer remains attached to the wall, the angle of inclination may be used to define the effective gravitational component in the direction of flow, $g_{eff} = g\ \mathrm{Cos}\ \theta$, and Eq. 14 becomes

$$Gr^*(x,\alpha,\theta) = g\mathrm{Cos}\theta[\rho_w - (1-\alpha)\rho_{f\infty}]\rho_f x^3/\mu_f^2 \tag{15a}$$

If $\alpha\rho_{f\infty} >> \rho_w - \rho_{f\infty}$, this reduces to the simple form below:

$$Gr^*(x,\alpha,\theta) \simeq \frac{g\mathrm{Cos}\theta\ \alpha x^3}{\nu_f^2} \tag{15b}$$

The experimental data of Gustavson, et al. were correlated on the basis of modified single-phase natural convection theory of the form indicated below,

$$Nu(x) = K_1[Gr^*(x,\bar{\alpha}) \cdot Pr]^{0.25} \tag{16a}$$

and

$$Nu(x) = K_2[Gr^*(x,\alpha) \cdot Pr]^{0.25} \tag{16b}$$

in which the properties used were the measured properties for the zinc sulfate solution at the appropriate film temperature. The value K_1 was determined from a log-linear least-squares fit to the data, and the forms of the correlations are

$$Nu(x) = .78[Gr^*(x,\bar{\alpha}) \cdot Pr]^{0.25} \tag{17a}$$

and

$$Nu(x) = .76[Gr^*(x,\alpha) \cdot Pr]^{0.25} \tag{17b}$$

The experimental data, as well as the log-linear least squares fit to the data as performed in Eq. 17a are shown in Fig. 2. The scatter in the correlation was basically the experimental scatter, and no finer structure was observed. The data appeared to behave similar to laminar natural convection and fell in the range $Ra^* < 10^{11}$ for the most part. As demonstrated in Eqs. 16a,b, the magnitude of the coefficient, K_1, was not a sensitive function of the void fraction [i.e., use of $\bar{\alpha}$ vs $\alpha(x)$]. The use of the average void fraction, $\bar{\alpha}$, was attractive since it eliminated the requirement of detailed knowledge of the local void distribution, $\alpha(x)$, which is significantly more difficult to measure and compute.

In order to use this correlation to predict the effects of boundary heat transfer from volume-heated boiling pools, knowledge of the pool-average void fraction, as seen in Eq. 16b, is required.

The void distribution may be calculated based on a one-dimensional two-phase drift flux model [1]. Consider a volume-heated boiling pool in which the volumetric vapor source may be written as

$$\Gamma_v = \frac{\dot{Q}_B'''(1-\alpha)}{h_{fg}} \tag{18}$$

where the term $(1-\alpha)$ signifies that the local heat generation occurs only in the liquid and Γ_v is the vapor source (gm/cm^3 sec). For most low power boiling pools in which the evaporated liquid is "made-up," the liquid volume flux will be negligible in comparison to the vapor volume flux. The steady state vapor mass conservation equation may be written as

$$\frac{dj_g}{dx} = \frac{\dot{Q}_B'''(1-\alpha)}{\rho_v h_{fg}} \tag{19}$$

The relation between the superficial vapor velocity, j_g, and the drift velocity, V_{gj}, may be written as [6],

$$\frac{\langle j_g \rangle}{\langle \alpha \rangle} = C_o \langle j \rangle + v_{gj} \qquad (20)$$

where the notation < > indicates a cross-sectional area average quantity. If we assume $\langle j \rangle \sim \langle j_g \rangle$ and the distribution parameter $C_o = 1.2$, this reduces to

$$\langle j_g \rangle = \frac{\langle \alpha \rangle v_{gj}}{1 - C_o \langle \alpha \rangle} \qquad (21)$$

Assuming that the drift velocity, V_{gj}, can be represented as

$$v_{gj} = U_\infty (1 - \alpha)^n \qquad (22)$$

where n = 0 for churn-turbulent flow, and n = 2 for bubbly flow and dropping the bracket notation, Eq. 19 becomes

$$\frac{d}{d\xi} \left[\frac{\alpha(1-\alpha)^n}{1 - C_o \alpha} \right] = K(1 - \alpha) \qquad (23)$$

subject to the initial condition

$$\alpha = 0 \text{ at } \xi = 0 \qquad (24)$$

where $\xi = x/H_o$ and $K = \frac{\dot{Q}_B''' H_o}{\rho_v h_{fg} U_\infty} = j_{g\infty}/U_\infty$. Equation 23 has been numerically integrated by two algorithms, an Euler predictor-corrector method and a fourth order Runge-Kutta method, with good agreement. The average void fraction, $\bar{\alpha}$ is defined as

$$\bar{\alpha} = \frac{\xi_{max} - 1}{\xi_{max}} \qquad (25)$$

The results of the local void fraction calculation were compared to the local void fraction data of Gustavson, et al., for four selected experimental runs for a value of K = 1.75. Although agreement between calculation and experiment was poor on a local basis, the average void fraction for the four runs, $\bar{\alpha}_{meas} \sim .40$, agreed quite well with the calculated average void fraction, $\bar{\alpha}_{calc} \sim .41$.

Although the data of Gustaveon, et al. tend to support the concepts of boundary layer heat transfer and one-dimensional drift flux two-phase vapor distribution modeling for pools in the bubbly flow regime, the uncertainty in the measurements performed make it difficult to differentiate the degree of agreement with the various models proposed, as well as to identify the various flow regime transition criteria for hydrodynamic and heat transfer behavior. In particular, the conditions for transition from bubbly flow to churn-turbulent flow are not clear, nor are the changes in the associated hydrodynamic and heat transfer behavior. As a result, it is difficult to extrapolate these results to other heat transfer systems of interest, in particular the behavior of internally-heated boiling pools of nuclear fuel in an HCDA, which may exist at power levels beyond the range of the previous work. For these reasons, the experiment described herein was undertaken.

EXPERIMENT

Pool Description

A schematic view of the overall pool construction is seen in Fig. 3. The pool was rectangular in cross-section, 18 cm wide x 33.5 cm long. The electrodes were recessed into lexan walls and polished to eliminate surface nucleation. The electrodes, as well as the walls and base, may be supplied with cooling water flow to eliminate preferential surface nucleation if necessary. Evaporative and boiling vapor losses were recovered through a make-up water flow port connected to a constant level weir adjusted to H_o. The net make-up water flow rate was measured and converted to gross vaporization power. The make-up flow was introduced from the pool bottom into a baffled space to pre-heat the water to T_{sat} and prevent inlet subcooling effects. No boiling occurred in this space. The entire pool was constructed of lexan with the exception of the copper electrodes and boron nitride test plate.

The boiling and nonboiling depths of the pool were measured with a voltage probe connected to a precision traversing mechanism. The conductor was lowered by the traversing mechanism until continuity was achieved and the voltmeter indicated the pool voltage. The pool was powered to the operating power and the probe was once again lowered until the operating voltage was again indicated. In this fashion, visual observations of pool depth were eliminated and more objective measurement of H_o and H_B was possible. The uncertainty in this measurement was essentially the fluctuation in pool height while boiling.

Test Plate

The test wall was constructed of lexan and was machined in such a fashion that the base of the test wall was continuously inclinable from the vertical position to any inclined position. The test surface was composed of boron nitride sheet (12.7 cm x 30.5 cm x 43 cm), machined and recessed into the lexan wall with the pool-side surface flush with the lexan and in direct contact with the boiling pool. The material has heat transfer characteristics of an excellent thermal conductor, but is electrically insulating at the same time. These properties, along with low water absorption and thermal expansion and ease of machining, made BN an ideal material for these tests. In addition, no electrically-insulating covering was necessary, eliminating contact heat transfer resistance and temperature extrapolation. The back surface of the BN test plate was cooled by flowing water. A separate flow loop was designed to supply a continuous flow of water, 15-20 lpm, to remove the heat transfered to the wall. The flow rate was designed to be high enough that the convective resistance to heat transfer in the coolant loop was negligible. The entire back surface of the BN was exposed to the coolant flow. This eliminated channel coolant effects, as well as hot and cold spots from coil cooling techniques.

Test Plate Instrumentation

The BN was instrumented with chromel-alumel thermocouples for local heat transfer measurements. The thermocouples were 0.0254 cm diameter stainless steel-clad microthermocouples, which were machined flat at the junction and electro-gold-plated with 0.00254 cm of gold forming the hot junction across the isolated chromel and alumel leads. A schematic

f the cross-sectionally polished and gold-plated icrothermocouples is shown in Fig. 4. The thermo- ouples were individually calibrated at the ice point nd steam point taking local barometric pressure into ccount, and the average calibration data for each as compared to NBS type K data. It was found that 11 the gold-plated thermocouples calibrated to ithin ± .07 °C from the steam to the ice point. he gold-plated microthermocouples were then cemented nto 26 locations in the BN wall, 19 on the front at .27 cm intervals, and 7 on the back at 3.81 cm ntervals. They were installed in such a manner that he measuring junction was flush with the wall urface within an estimated ± .0025 cm tolerance and emented in place under a microscope. The gold- lated junction thus comprised part of the test wall urface. Heat losses along the thermocouple sheath ere negligible since the leads were immersed in the late at least 50 diameters.

ata Acquisition

The thermocouples were connected to a 150 °F ± 2 °F oven-type reference junction along with a hermocouple in the bulk pool, and the data was then outed to the automated data acquisition system. The entralized data acquisition and analysis system was onstructed around an HP 9640 system, consisting of a 1 MX minicomputer with 112 kilowords of central emory, 7.5 megaword cartridge disk, and 9 track agnetic tape transport. Control of the system was ccomplished by interactive software, which received ransfer parameters from the experimenter and pro- eeded to scan the data channels upon command. The hermocouples were scanned by a 300 channel guarded rossbar acenner, which transfered data to an inte- rating digital voltmeter with microvolt resolution. ach thermocouple was sequentially sampled until the tandard deviation of the output converged to a reset criterion or the maximum sample limit was xceeded. At this point, the scanner proceeded to he next thermocouple and repeated the same procedure ntil all 27 thermocouples had been integrated. The au data was transferred to magnetic tape and preli- nary engineering calculations were performed to onvert the thermocouple output and system properties nto local convective heat transfer coefficient and verage pool void fraction.

ESULTS

The experiments have been performed over a range f volumetric vaporization power up to $j_{g_\infty}/U_\infty = 1$. ocal heat fluxes along the inclined boundary were easured as indicated in Eq. 26

$$h(x) = \frac{k_{BN}(T_{front}(x) - T_{back}(x))}{a \cdot (T_{pool} - T_{front}(x))} \qquad (26)$$

ccuracy of these measurements is estimated to be ithin ± 5 percent. The tests reported herein do not ave local void fraction measurements included, but ather are correlated only on an overall average asis. The pool-average void fraction was measured s indicated in Eq. 27.

$$\bar{\alpha} = (H_B - H_o)/H_B \qquad (27)$$

ith an estimated accuracy of ± 3 percent.

For the boiling experiments presented here, the wall angles investigated were 90° ± .5° (vertical) and 75° ± .5°. The local boundary boiling heat transfer coefficients measured indicated a spatial distribution similar to the behavior suggested by the boundary layer analyses in Eqs. 10 and 17. A typical profile of local boundary heat transfer coefficient from a volume-boiling pool in the bubbly flow regime is presented in Fig. 5 and compared to the predic- tions of Eq. 10 and 17. In the bubbly flow regime, the local heat transfer coefficient was seen to be greatest at the pool surface (x = 0) and decrease monotonically as the depth increased. In addition, it was evident that the local convective heat flux varied by a factor of 3 in this case, and has been seen to vary by as much as a factor of 5 or more along the boundary in other cases. This was in contrast to the spatial variation of a factor of 1.5 to 2 reported previously [2,4]. Comparison of the local heat transfer coefficient distribution for these experiments to those reported by Gustavson [2] indicate that the present measurements exceed the previous measurements in magnitude by as much as a factor of 2.

The local heat transfer distribution was inte- grated to yield the average heat transfer coefficient defined as

$$\bar{h} = \frac{1}{L}\int_0^L h(x)dx \qquad (28)$$

The average heat transfer data for 9000, 7500, and 6000 series runs (indicating the wall angle measured from horizontal) are presented in Table 1 and com- pared to the calculations of Eq. 17 and Eq. 10 (for n = 0.7 and 1.0). The data confirm that the experi- mentally measured average heat transfer coefficients exceed the predictions of both heat transfer rela- tions available (derived from Gustavson's data) by a factor of approximately 2. The detailed local data also confirm this observation. The best agreement was achieved with Eq. 17.

The average void fraction data were correlated as a function of the dimensionless superficial vapor velocity, j_{g_∞}/U_∞, and are presented in Fig. 6. The dimensionless superficial vapor velocity was based on the total vaporization power applied to the pool, which includes the evaporative losses, as well as boiling losses. The data indicate that for the bubbly flow regime, $\bar{\alpha}$ is a very sensitive function of the power, and small changes in power may cause large variations in $\bar{\alpha}$. Reproducibility is indicated by the over-lapping data points, and agreement is excellent.

A threshold value of j_{g_∞}/U_∞, below which the pool will be volume-heated but nonboiling, has been observed previously and is also seen here. This indicates the magnitude of the evaporative losses from the pool and is subtracted from the applied vaporization power to yield the net power for boiling indicated below

$$(j_{g_\infty}/U_\infty)^* = j_{g_\infty}/U_\infty - (j_{g_\infty}/U_\infty)_o \qquad (29)$$

It is observed that for the range of j_{g_∞}/U_∞ in which the void fraction is less sensitive to the power, this correction is negligible. This will be particularly true in the churn-turbulant flow regime. Equation 23 was solved for $\bar{\alpha}^*$ corresponding to

$(j_{g_\infty}/U_\infty)^*$ (net boiling power) and bubbly flow. The measured and calculated average void fractions are presented in Table 1 and Fig. 7. It is observed that the calculated average void fraction data predict the experimental data well when based on the true boiling power density, $(j_{g_\infty}/U_\infty)^*$, and that the agreement improves for increasing α. The distribution of average void fraction as a function of dimensionless superficial vapor velocity indicates that the bubbly flow exists up to j_{g_∞}/U_∞ approximately equal to unity. Flow regime transition to churn-turbulent flow occurs at higher value of j_{g_∞}/U_∞; the pool behavior becomes chaotic, and the average void fraction is observed to collapse from approximately 0.60 to approximately 0.40. The boundary layer-type nature of the boiling heat transfer coefficient appears to be replaced by a more nearly uniform distribution spatially, which experiences large fluctuations temporally.

CONCLUSIONS

For volume-heated boiling pools characteristic of the kind investigated here and in the bubbly flow regime, the following conclusions can be made:

(1) Boundary heat transfer from volume-boiling pools in the bubbly flow regime behaved similar to natural convection-type boundary layer heat transfer. The spatial variation in the local heat transfer coefficient was as great as a factor of 3-5 along the wall, with the greatest heat transfer at or near the pool surface. The data reported here for local convective heat transfer coefficient exceeded those previously reported [2] by a factor of 2 or more.

(2) For boundary layer-type heat transfer from volume-boiling pools in the bubbly flow regime, the effect of small angle of inclination of the boundary from vertical was modeled by defining an effective gravitational component along the wall as indicated below:

$$g_{eff} = g \cos\theta \qquad (30)$$

where θ is the angle of inclination from the vertical.

(3) The bubbly flow regime persisted for a value of j_{g_∞}/U_∞ up to unity. In this flow regime, the pool underwent periodic swelling due to subcooling from the returning cold boundary layer fluid into the pool bottom. The pool exhibited a stratified state with a boiling region over an essentially nonboiling single phase region below. The depth of the nonboiling region decreased as the volumetric vaporization source increased.

(4) The maximum average void fraction observed in bubbly flow regime was in the range of 0.55 to 0.60 at j_{g_∞}/U_∞ approximately unity. In this range of power, transition to a churn-turbulent flow regime was observed in which boiling penetrated to the pool bottom, and a sudden collapse in average pool void fraction was observed from approximately 0.55-0.60 to 0.40.

(5) In the bubbly flow regime, it was observed that surface evaporative losses were nonnegligible for pools with large surface-to-volume ratio, and that a significant fraction of the volumetric power density went into these losses. The net boiling power was defined as the total vaporization power minus the evaporative losses. It was found that calculation of the pool-average void fraction by means of a one-dimensional drift flux model based on the net boiling power agreed well with the experimental data independent of the wall angle. Agreement between calculated and measured average void fraction improved for increasing power.

(6) The average void fraction in the bubbly flow regime was found to be very sensitive to the volumetric boiling power. Small changes in j_{g_∞}/U_∞ were observed to cause large variations in the pool-average void fraction.

REFERENCES

1 Greene, G. A., Jones, O. C., Jr., and Schwarz, C. E., "Thermo-Fluid Mechanics of Volume-Heated Boiling Pools," Third PAHR Information Exchange, Argonne National Laboratory, ANL-78-10, BNL-NUREG-50759, (November 1977).

2 Gustavson, W. R., Chen, J. C., and Kazimi, M. S., "Heat Transfer and Fluid Dynamic Characteristics of Internally Heated Boiling Pools," BNL-NUREG-50722 (September 1977).

3 Stein, R. P., Hesson, J. C., and Gunther, W. H., "Studies of Heat Removal From Heat Generating Boiling Pools," ANS Fast Reactor Safety Conference, CONF-740401, pp 865-880 (April 1974).

4 Gabor, J. D., Baker, L., Jr., Cassulo, J. C., and Mansoori, G. A., "Heat Transfer from Heat Generating Boiling Pools," ASME-AIChE National Heat Transfer Conference, St. Louis, MO, pp 78-80 (1976).

5 Churchill, S. W. and Usagi, R., "A General Expression for the Correlation of Rates of Transfer and Other Phenomena," AIChE, 18, n-6, pp. 1121-1128 (1972).

6 Zuber, N. and Findlay, J. A., "Average Volumetric Concentration in Two-Phase Flow Systems," J. Heat Transfer, pp. 453-468 (November 1965).

9-369-76

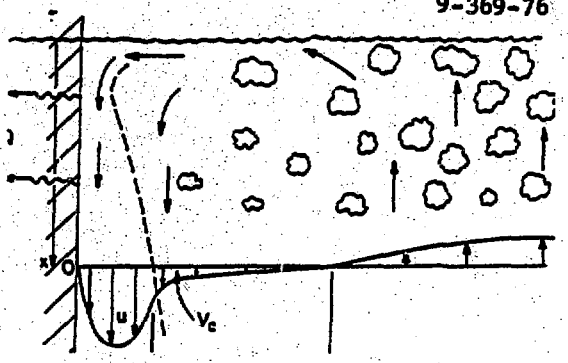

Fig. 1 Schematic of Boundary Layer Flow and Heat Transfer from Volume-Heated Boiling Pools.

1-1385-79

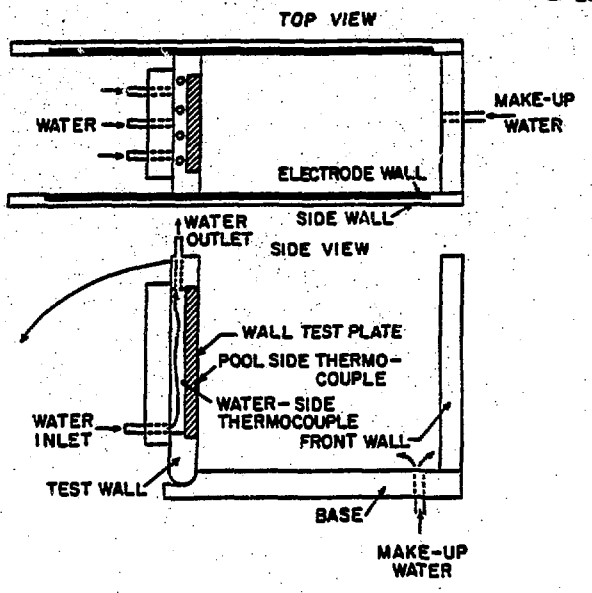

Fig. 3 Schematic View of Volumetric Boiling Pool Apparatus.

1-1295-79

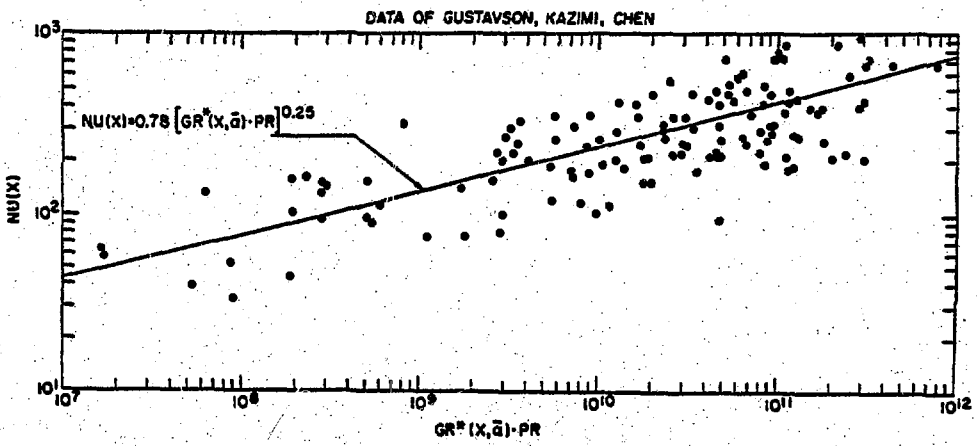

Fig. 2 Modified Laminar Natural Convection Correlation of Local Boundary Heat Transfer From Volumetric Boiling Pools.

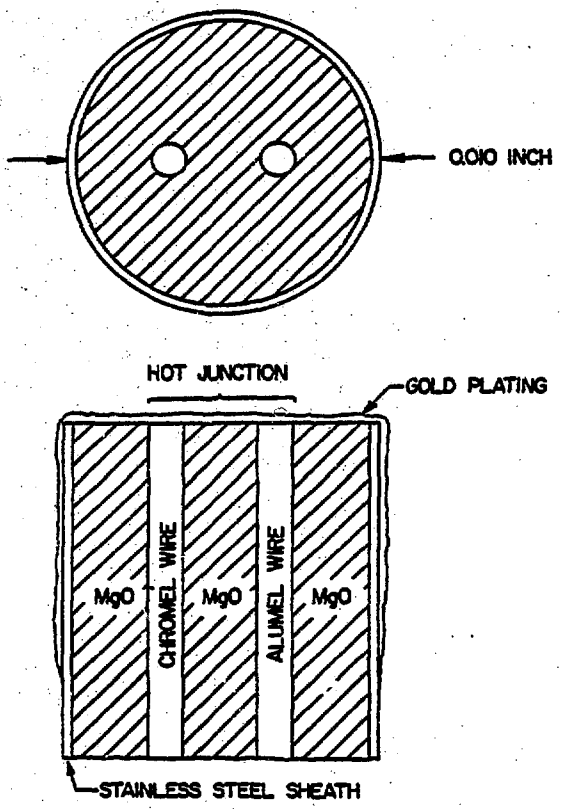

Fig. 4 Schematic View of Gold-Plated Microthermocouple.

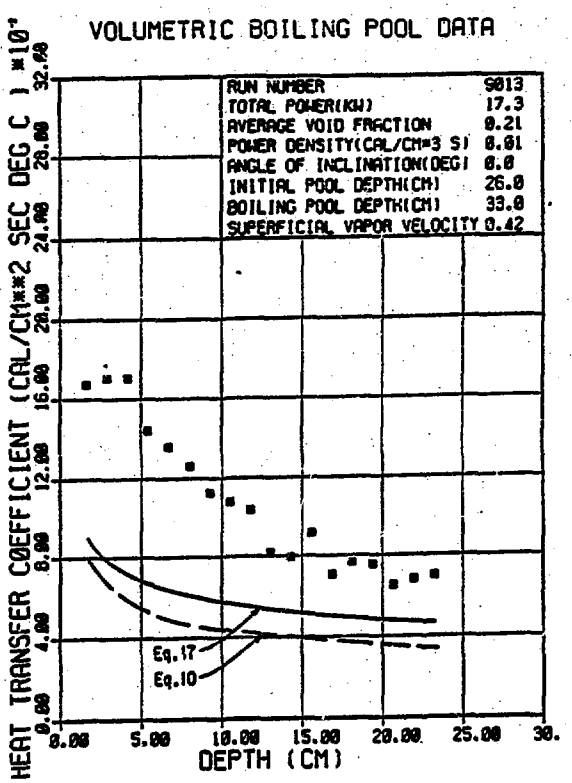

Fig. 5 Spatial Distribution of Heat Transfer Coefficient from Volume Boiling Pool in Bubbly Flow Regime.

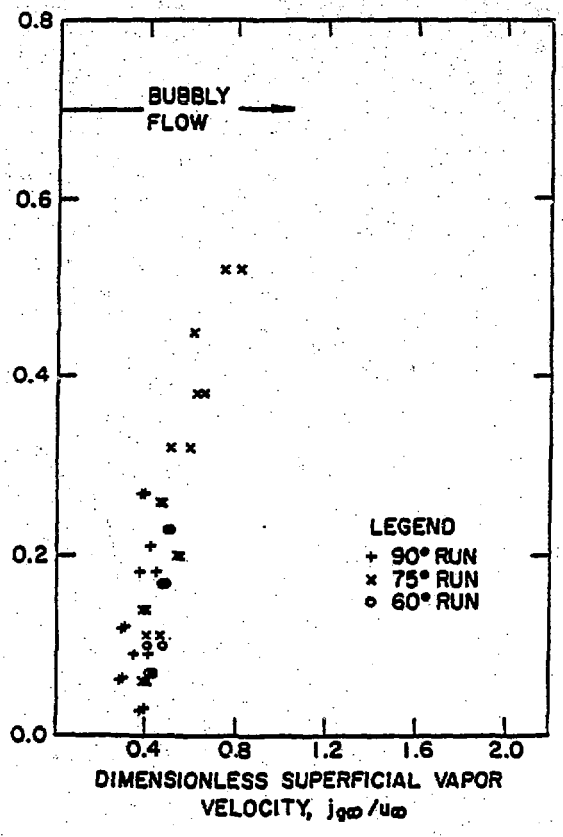

Fig. 6 Pool-Averaged Void Fraction in the Bubbly Flow Regime vs. Dimensionless Superficial Vapor Velocity Based Upon Total Vaporization Power.

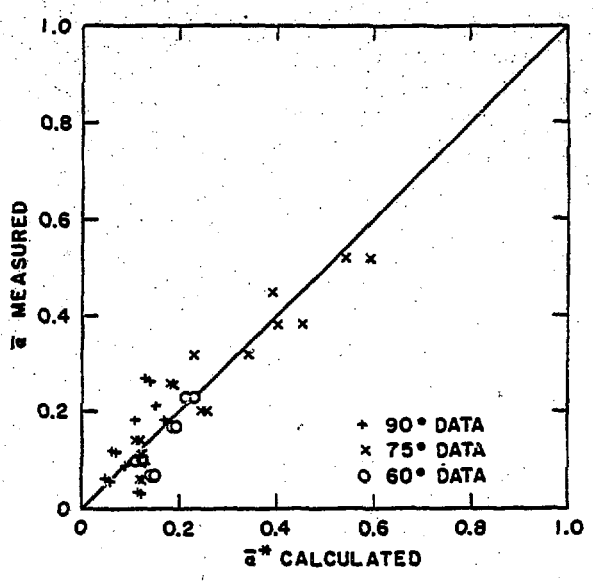

Fig. 7 Comparison of Measured and Calculated Average Void Fraction Based Upon Net Boiling Power.

TABLE I

COMPARISON OF DATA TO MODEL CALCULATIONS FOR AVERAGE VOID FRACTION AND HEAT TRANSFER COEFFICIENT

RUN	WALL TEMP DEG C	VOID FRACTION EXP	VOID FRACTION CALC	AVERAGE HEAT TRANS COEFF CAL/CM2 S DEG C EXP	EQ 17	EQ 10 N=1.0	EQ 10 N=0.7	SVV
9001	82.3	.03	.12	.054	.037	.037	.047	.39
9002	83.1	.03	.12	.056	.037	.037	.047	.38
9003	83.5	.06	.05	.063	.044	.038	.049	.28
9004	83.8	.06	.05	.064	.044	.038	.049	.28
9005	84.2	.09	.13	.072	.049	.044	.056	.41
9006	84.2	.09	.09	.072	.049	.043	.054	.35
9007	85.9	.12	.08	.081	.053	.044	.055	.30
9008	86.9	.13	.08	.085	.053	.044	.055	.30
9009	88.5	.18	.11	.104	.059	.048	.062	.32
9010	88.5	.18	.17	.109	.059	.058	.064	.45
9011	89.8	.17	.13	.121	.065	.052	.066	.38
9012	89.8	.17	.13	.128	.065	.053	.068	.38
9013	89.1	.21	.15	.105	.061	.051	.065	.42
7501	84.7	.11	.12	.079	.051	.046	.058	.46
7502	85.9	.11	.12	.079	.051	.045	.057	.46
7503	85.7	.14	.12	.088	.055	.046	.059	.39
7504	85.6	.14	.11	.081	.055	.046	.059	.38
7505	88.5	.20	.21	.106	.068	.052	.066	.54
7506	88.4	.20	.20	.104	.068	.052	.066	.52
7507	89.8	.26	.24	.115	.074	.053	.067	.59
7508	89.4	.26	.24	.112	.074	.053	.067	.59
7509	90.8	.32	.24	.121	.080	.057	.073	.53
7510	91.1	.32	.23	.131	.080	.056	.071	.51
7511	91.7	.32	.23	.138	.081	.058	.076	.51
7512	91.9	.38	.25	.131	.081	.060	.076	.55
7513	92.3	.45	.39	.148	.074	.061	.077	.81
7514	93.2	.44	.34	.168	.078	.066	.084	.71
7515	92.7	.52	.39	.159	.078	.057	.085	.81
7520	82.9	.06	.12	.064	.045	.042	.053	.46
7521	82.3	.06	.12	.072	.045	.042	.053	.46
6001	83.4	.07	.15	.087	.045	.041	.052	.43
6002	83.4	.17	.19	.103	.057	.048	.061	.44
6003	83.4	.07	.15	.080	.045	.041	.052	.43
6004	83.5	.17	.19	.091	.057	.048	.061	.44
6005	83.2	.10	.12	.088	.051	.044	.056	.46
6006	83.0	.10	.11	.083	.052	.045	.058	.48
6007	83.4	.21	.21	.120	.064	.054	.069	.56
6008	83.7	.20	.21	.130	.064	.054	.069	.51